Genes & Diseases (2023) 10, 568–582

Available online at www.sciencedirect.com

ScienceDirect

journal homepage: www.keaipublishing.com/en/journals/genes-diseases

FULL LENGTH ARTICLE

Zinc-finger protein 382 antagonises CDC25A and ZEB1 signaling pathway in breast cancer

Shuman Li [a,b,1], Xiaoqian He [c,1], Yan Wang [c], Weihong Chen [c], Ran Sun [c], Shaorong Tian [c], Sanxiu He [c], Chunyun Pu [c], Chen Li [d], Dishu Zhou [c], Yu Jiang [c], Qian Tao [d], Lili Li [d], Lin Ye [c], Yue Wu [c], Weiyan Peng [c], Tingxiu Xiang [b,c,*]

[a] *Department of Oncology, The Second Affiliated Hospital of Chongqing Medical University, Chongqing 400016, China*
[b] *Chongqing Key Laboratory of Translational Research for Cancer Metastasis and Individualized Treatment, Chongqing University Cancer Hospital, Chongqing 400030, China*
[c] *Key Laboratory of Molecular Oncology and Epigenetics, The First Affiliated Hospital of Chongqing Medical University, Chongqing 400016, China*
[d] *Cancer Epigenetics Laboratory, Department of Clinical Oncology, State Key Laboratory of Translational Oncology, Sir YK Pao Center for Cancer, Li Ka Shing Institute of Health Sciences, The Chinese University of Hong Kong and CUHK Shenzhen Research Institute, Shenzhen, Guangdong 518172, China*

Received 24 May 2021; received in revised form 13 November 2021; accepted 22 December 2021
Available online 9 February 2022

KEYWORDS
Breast cancer;
CDC25A;
EMT;
ZEB1;
ZNF382

Abstract Our previous studies found that Zinc-finger protein 382 (ZNF382) played as a tumor suppressor gene in esophageal and gastric cancers, and a positive correlation between the high expression of ZNF382 and better outcome in breast cancer patients. However, the biological roles and mechanisms of ZNF382 in breast cancer remains unclear. We detected ZNF382 expression by reverse-transcription PCR (RT-PCR) and real-time quantitative PCR (qRT-PCR) in breast cancer cells and tissues, and explored the impacts and mechanisms of ectopic ZNF382 expression in breast cancer cells *in vitro* and *in vivo*, respectively. Our results revealed that ZNF382 was significantly down-regulated in breast cancer tissues compared with adjacent non-cancer tissues. Restoration of ZNF382 expression in silenced breast cancer cells not only inhibited tumor cell colony formation, viability, migration and invasion, and epithelial-

* Corresponding author. Chongqing Key Laboratory of Translational Research for Cancer Metastasis and Individualized Treatment, Chongqing University Cancer Hospital, Chongqing 400030, China. Fax: +86 23 65079282.
E-mail address: xiangtx@cqmu.edu.cn (T. Xiang).
Peer review under responsibility of Chongqing Medical University.
[1] These authors have contributed equally to this work.

https://doi.org/10.1016/j.gendis.2021.12.019

mesenchymal-transition (EMT), but also induced apoptosis and G0/G1 arrest. In conclusion, ZNF382 could induce G0/G1 cell cycle arrest through inhibiting CDC25A signaling, and, inhibit cell migration, invasion and EMT by antagonizing ZEB1 signaling in breast cancer cells.

Introduction

Breast cancer is one of the most common malignant tumors in women and the incidence is increasing year by year.[1] Treatments including Herceptin and everolimus play important roles in breast cancer comprehensive therapy.[2–4] For triple-negative breast cancer, new drugs also have been developed, such as PD1/PDL1 monoclonal antibody, ramolutumab, and so on.[5,6] However, molecular targeted therapy for breast cancer is still very limited.[7,8] Therefore, identification of novel effective biomarkers and molecular mechanism is vital to increasing breast cancer survival and treatment efficacy.[9]

Krüppel-associated box (KRAB)-containing zinc-finger protein (KZNF) is a C2H2 zinc-finger protein which involved in multiple biological processes including cell differentiation, proliferation, apoptosis and tumorigenesis.[10] KRAB domain, a protein—protein interaction region, can be combined with multiple synergistic factors, such as transcription inhibitor heterochromatin protein 1(HP1) and KRAB associated protein 1(KAP1).[11,12] In addition, it can bind to histone deacetylase active factors to form complexes. C2H2 zinc finger domains play a regulatory role by binding with downstream DNA and are regulated by the complex formed in the KRAB region.[13] KZNF family usually plays a transcriptional regulatory role, inhibiting downstream signaling pathways.[10]

Zinc finger protein 382 (ZNF382), as a member of KZNF family, located in Chromosome 19q13.12, had abnormal promoter region methylation and downregulated expression in a variety of tumors.[13–15] While KRAB domain can play a synergistic role in KAP1 inhibition, it has been found that ZNF382 can inhibit the activator protein-1 (AP-1) and nuclear factor (NF)-κB signaling pathways as a tumor suppressor gene in multiple carcinoma types.[13,14,16] In gastric cancer, promoter hypermethylation contributed to downregulate ZNF382, and ZNF382 turned out to be a tumor suppressor gene (TSG) by inhibiting tumor cell growth and metastasis.[15] In oesophageal squamous cell carcinoma, ZNF382 was inactivated by promoter CpG methylation, and suppressed Wnt/β-catenin signaling via binding directly to promoters of FZD1 and DVL2.[14] In HBV-related hepatocellular carcinogenesis, ZNF382 could transcriptionally repress its downstream targets such as Fos proto-oncogene (FOS), Jun proto-oncogene and impair the activities of AP-1 and activating p53 signaling.[16] In pediatric acute myeloid leukemia, patients with ZNF382 methylation showed lower ZNF382 transcript levels.[17] All these evidences indicated that aberrant promoter CpG methylation results in ZNF382 down regulation in multiple carcinoma types and ectopic expression of ZNF382 suppressed tumor cell proliferation and promotes apoptosis. However, the role of ZNF382 in breast cancer remains uncertain. In the current study, we focused on the functions and mechanisms of ZNF382 in breast cancer *in vitro* and *in vivo*, revealing ZNF382 may be a potential target for breast cancer treatment.

Materials and methods

Cell culture and tissue samples

Breast cancer cell lines used in this study included MDA-MB231, MCF-7 and BT549, which were acquired from the American Type Culture Collection (ATCC; Manassas, VA, USA). Cells were cultured in the RPMI-1640 medium (Gibco-BRL, Karlsruhe, Germany) at 37 °C and 5% CO_2 supplemented with 100 mg/mL streptomycin, 100 U/mL penicillin, and 10% fetal bovine serum (FBS, Gibco-BRL). All breast cancer tissues and paired surgical margin tissues were obtained after surgical procedures conducted at the First Affiliated Hospital of Chongqing Medical University, Chongqing, China. All clinical samples were subjected to histological diagnosis by pathologists and informed consent were obtained from patients for acquisition of tissue specimens. This study was approved by the Ethics Committee of the First Affiliated Hospital of Chongqing Medical University (approval notice: 20120307).

Establishment of stable cell lines

To establish stable cell lines with ZNF382 expression, MCF-7 and MDA-MB231 cells were plated into six-well plates and transfected with pcDNA3.1-ZNF382-Flag or pcDNA3.1 plasmid (4 μg/well) using Lipofectamine™ 2000 (Invitrogen Carlsbad, CA, USA). After 48 h, transfected cells were then cultured with selective medium containing G418 (50 mg/mL) for 14 days, 4 μL/mL for MCF-7 and 24 μL/mL for MDA-MB-231 cells. RT-PCR and Western blot analysis were used to test the efficiency of ZNF382 overexpression prior to performing other experimental procedures.

RNA extraction, RT-PCR, qPCR and methylation specific PCR (MSP)

Total RNA was extracted from cell lines and tissues using the TRIzol Reagent (Invitrogen) while following the manufacturer's instructions. Aliquots containing 1 μg of total RNA were reverse-transcribed in 20 μL of cDNA. Samples were stored at −20 °C for further use. RT-PCR was performed using Go-Taq (Promega, Madison, WI, USA) with initial denaturation at 95 °C for 2 min, and followed by 32 cycles (95 °C for 30 s, 55 °C for

30 s, and 72 °C for 30 s) of amplification, with a final extension at 72 °C for 3 min. β-actin was amplified as an internal control for 23 cycles. qPCR was amplified by using the SYBR® Green Master Mix (Applied Biosystems, Grand Island, NY, USA) according to the manufacturer's instructions. Moreover, all experiments were performed in triplicate. MSP were carried out as previously described. Primer sequences are listed in Table 1 and Table 2.

Cell viability assays

Cells stably expressing ZNF382 or vector were seeded in 96-well plates (5000 cells per well). Proliferation was measured with the Cell Counting Kit-8 (CCK-8, Beyotime, Shanghai, China) according to the manufacturer's introductions. Absorbance was measured after 24, 48, and 72 h at 450 nm with a microplate reader (Multiskan MK3, Thermo Fisher Scientific, Germany). All experiments were independently repeated three times.

Colony formation assays

MDA-MB231 and MCF7 cells stably expressing ZNF382 or vector had been seeded in six-well plates at densities of 200, 400, and 800 cells/well with G418 selection for 2 weeks. Colonies with more than 50 cells per colony were fixed in 4% formalin and stained with gentian violet. All independent experiments were performed in triplicate.

ZNF382 knockdown in cell lines

To further explore the function of ZNF382, the effect of ZNF382 was tested via ZNF382 knockdown in BT549 cells using siRNA (OriGene Technologies) or shRNA (Chloramphenicol, TL330228) transfection. All transfections were performed by using Lipofectamine 2000 (Invitrogen) according to the manufacturer's instruction with siRNA concentration of 50 nM. Cells collected after 72 h of transfection. Knockdown efficiency was detected by RT-PCR and qPCR.

Wound healing, transwell migration, and invasion assays

Stable cell lines with ZNF382 or vector-expressing MDA-MB-231 cells were seeded in six-well plates and cultured until single layer confluence was achieved. A linear scratch was made by using a pipette tip and cell migration distance was measured at different times with a comparative microscope (Leica DMI4000B, Milton Keynes, Bucks, UK).

Table 1 List of PCR primers used in this study.

PCR	Primer	Sequence (5′-3′)	Product size (bp)	PCR Cycles	Annealing temperature (°C)
RT-PCR	*ZNF382F*	CCTTACAGGGATCAGTGTCA	173bp	32	55
	ZNF382R	CAACTTGCGGATCATATCAG			
	GAPDHF	GGAGTCAACGGATTTGGT	206bp	23	55
	GAPDHR	GTGATGGGATTTCCATTGAT			
qRT-PCR	*CDK1F*	CGCAACAGGGAAGAACAG	135bp		60
	CDK1R	CGAAAGCCAAGATAAGCAAC			
	CDK2F	GAAACAAGTTGACGGGAGA	238bp		60
	CDK2R	AGAGGAATGCCAGTGAGA			
	CDK4F	CGGTGCCTATGGGACAGT	179bp		60
	CDK4R	GCCGGACAACATTGGGAT			
	CDK6F	AACCACCCAAGATGACC	107bp		60
	CDK6R	TGTGGACAAGCCAGGATG			
	c-MycF	GGAGGCTATTCTGCCCATTT	177bp		60
	c-MycR	GTCGAGGTCATAGTTCCTGTTG			
	CDC25AF	ACCAACCTGACCGTCACTAT	220bp		60
	CDC25AR	GACTACATCCCAACAGCTTAG			
	MYCF	CTCTCCGTCCTCGGATTCTC	211bp		60
	MYCR	GCCTCCAGCAGAAGGTGATC			
	NANOGF	ATGAGTGTGGATCCAGCTTG	190bp		60
	NANOGR	CCTGAATAAGCAGATCCATGG			
	OCT4F	AGCGATCAAGCAGCGACTAT	118bp		60
	OCT4R	TAGCCTGGGGTACCAAAATG			
	SOX2F	TCTTCGCCTGATTTTCCTCGCG	178bp		60
	SOX2R	CAGCTCCGTCTCCATCATGTTGT			
	Snail1F	GAGGCGGTGGCAGACTAG	159bp		60
	Snail1R	GACACATCGGTCAGACCAG			
	VimentinF	GACCAGCTAACCAACGACAA	150bp		60
	VimentinR	GTCAACATCCTGTCTGAAAGAT			
	occludinF	ATGTGCATTGCCATCTTTGCCTG	138bp		60
	occludinR	ATAGCCATAGCCACTTCCGTAG			

Note: RT-PCR: Reverse Transcription-Polymerase Chain Reaction, qPCR: quantitative Polymerase Chain Reaction.

Table 2 MSP and Chip-PCR primers used in this study.

PCR	Primer	Sequence (5′-3′)	Product size (bp)	PCR Cycles	Annealing temperature (°C)
MSP	ZNF382m1	GGCGATTAACGGGTCGTTTC	bp	40	60
	ZNF382m2	AAAATTTCCAAACCCGACTCG			
	ZNF382 u1	GTGGTGATTAATGGGTTGTTTT	bp	40	58
	ZNF382 u2	CAAAATTTCCAAACCCAACTCA			
ChIP-qPCR	ZEB1F1	AAGGAGGCTGCTGGCAAGC	171bp		
	ZEB1R1	GGCGACCGGAGAGAGGCTA			
	ZEB1F2	GTAGCCTCTCTCCGGTCGC	150bp		
	ZEB1R2	TACCATCAGTCCCACGCCTCG			
	CDC25AF1	AGAGCCGATGACCTGGCAGA	118bp		
	CDC25AR1	ACGGAATCCACCAATCAGTAAG			
	CDC25AF2	GCTTACTGATTGGTGGATTCCG	194bp		
	CDC25AR2	GCTCACGCTGTCTTCGCTGT			
	CDC25AF3	GAACAGCGAAGACAGCGTGAG	260bp		
	CDC25AR3	CGGGTCAAACACAAACACGACT			

Cell migratory and invasive abilities were investigated by using Transwell and Matrigel invasion assays with two-chamber plates and a pore size of 8 μm (Corning, New York, NY, USA). Cells stably expressing ZNF382 or vector were seeded in the upper Transwell chambers (1×10^4 cells per chamber) in serum-free medium after being washed twice. About 800 μL of the culture solution with 20% FBS were added to the lower chambers. After cells migrated to the other side of the chamber, they were fixed and stained with 0.1% crystal violet and counted in five microscopic fields of view. Each experiment was performed in replicate inserts and the mean value was calculated from three independent experiments.

Immunofluorescence

MDA-MB231 and MCF7 cells were seeded in 24-well plates with micro cover glass and transfected with pcDNA3.1-ZNF382-Flag or pcDNA3.1 plasmid. After 48 h, cells were fixed with 4% paraformaldehyde for 30 min, permeabilized with 0.5% Triton X-100 for 10 min at room temperature, and then blocked with the blocking buffer. After treatment, slides were incubated with anti-FLAG M2 (#14793, Cell Signaling Technology, Danvers, MA), anti-E-Cadherin (1:200, sc-8426, Santa Cruz Biotechnology, CA, USA), and anti-N-Cadherin (1:200, #610921, BD Biosciences, CA, USA) antibodies at 4 °C. After 20 h, cells were incubated with Alexa Fluor 594- or 488-conjugated goat anti-mouse secondary antibodies (Jackson ImmunoResearch, West Grove, PA, USA) for 1 h at 4 °C in the dark. All slides were counterstained with 4′-6-diamidino-2-phenylindole (Roche, Palo Alto, CA, USA). Photomicrographs were captured with a confocal laser scanning microscope. All assays were performed three times.

Immunohistochemistry (IHC)

Tissue samples were processed as described above. IHC analysis was performed by using the UltraSensitive TM SP Kit (Maixin-Bio, Fujian, China) according to the manufacturer's instructions. Tissue slices were then incubated with the primary antibody (ZNF382, 1:50 dilution, HPA049259 Sigma; Ki67, 1:50, ARG53222 arigo; CDC25A 1:100, Cell Signaling Technology) overnight at 4 °C, flushed three times with phosphate-buffered saline (PBS), and incubated with the secondary antibody for 30 min at room temperature. Color development was performed with DAB and hematoxylin and eosin (H&E).

Cell cycle and apoptosis assays

Flow cytometry was used to assess to cell cycle and cell apoptosis. The MDA-MB231 and MCF7 cells were seeded in 6-well plates and transfected with pcDNA3.1-ZNF382-Flag or pcDNA3.1 plasmid, after 48 h, collecting cells,and BT549 cells were seeded and transfected with siRNA or siNC(control), after 48 h, collecting cells. The cell cycle and apoptosis were stained by PI or combined with Annexin V-fluorescein isothiocyanate and PI, respectively. Flow cytometry results were evaluated in triplicate by using the Cell Quest kit (BD Biosciences). All experiments were performed in triplicate.

Luciferase reporter assays

The effect of *ZNF382* on CDC25A transcriptional activity was studied by dual luciferase reporter assay. The pGL3/Basic plasmids which expressed the firefly luciferase reporter was used as a framework in ten generations of Reporter gene plasmids. We amplified the promoter region of the gene via PCR and cloned into the pGL3/Basic plasmid with a seamless cloning kit (D7010S, Beyotime, Beijing, China), which was then verified by sequencing. MCF7 cells were transiently co-transfected with a pGL3-CDC25A and pcDNA3.1-ZNF382-Flag or vector (pcDNA3.1) with a Renilla luciferase reporter pRL-TK (Promega) as an internal control. Then the dual-luciferase reporter assay kit (Promega) was used to test the luciferase activity after 48 hours. All experiments were performed in triplicate.

The regulation of Zinc finger E-box binding homeobox 1 (ZEB1) by ZNF382 was verified to be consistent with the above method through luciferase report experiment. Concrete primers are listed in Table 2.

Chromatin immunoprecipitation (ChIP) assay

Chromatin immunoprecipitation (ChIP) assay was executed as mentioned previously.[18] The antibodies used in this experiment were as follows: anti-Flag M2 (#14793, Cell Signaling Technology) and Normal rabbit IgG (#2729, Cell Signaling Technology). Concrete primers are listed in Table 2.

Western blotting

Western blotting was performed as described previously.[19] The primary antibodies used in this study were as follows: E-Cadherin (sc-8426; Santa Cruz Biotechnology), N-Cadherin (ab98952; Abcam), Occludin (sc-133255; Santa Cruz Biotechnology), SLUG (sc-166476; Santa Cruz Biotechnology), SNAIL (sc-271977; Santa Cruz Biotechnology), ZEB1 (sc-515797; Santa Cruz Biotechnology), β-actin (sc-47778; Santa Cruz Biotechnology), CDC2 (sc-54; Santa Cruz Biotechnology), p-CDC2 (sc-136014; Santa Cruz Biotechnology), CCND1 (sc-450; Santa Cruz Biotechnology), C-Myc (#13987; Cell Signaling Technology), GAPDH (bsm-0978 m; Biss), Ki67 (ARG53222; arigo), CDC25A (#Cell Signaling Technology), and Vimentin (sc-6260; Santa Cruz Biotechnology). The Immobilon Western Chemiluminescent HRP Substrate kit (Millipore Corporation, Billerica, MA, USA) was used to detect signal intensity of proteins.

Xenograft tumors in nude mice

Animal experiments were conducted to verify whether ZNF382 can inhibit tumor growth *in vivo*. Five female BALB/c nude mice (4—6 weeks old, weight 18—20 g) were obtained from the experimental animal center of the Chongqing Medical University. Stable MDA-MB231 cells with ZNF382 expression and control group cells (5×10^6 cells in 0.1 mL of PBS without serum) were subcutaneously injected into nude mice's bilateral posterior buttocks. The left side was used for the experimental group and the right side was used for the control group. Tumor diameters were measured every 4 days, 20 days in total. The BALB/c nude mice were sacrificed and their tumors were removed when the tumor length reached 1 cm. This study was approved by the Ethics Committee of the Chongqing Medical University, China.

Statistics

SPSS20.0 software (Chicago, IL) was used for statistical analyses. All data are presented as the mean ± SD. Student's *t*-test were used to analyze the significance of differences between the experimental and control values. χ^2 tests were used to compare the ZNF382 promoter methylation status with clinicopathological features. We used technical replicates for statistical analyses. The significance level was $P < 0.05$. $^*P < 0.05$; $^{**}P < 0.01$; $^{***}P < 0.005$.

Results

ZNF382 is downregulated in breast cancer cells and tissues

Low expression of ZNF382 was found in breast cancer tissues. ZNF382 expression was detected in breast cancer tissue samples and paired tumor-adjacent samples by IHC in 32 cases. IHC analysis showed that ZNF382 was downregulated in breast cancer specimens compared to the para-cancerous tissues (Fig. 1A). ZNF382 expression in breast cancer and adjacent tissues was detected by qPCR. To incorporate this outcome on a clinical level, these specimens were classified into luminal and basal groups according to their pathological features. ZNF382 demonstrated a relatively low expression in the basal group, whereas no significant difference was present in the luminal group (Fig. 1B). In addition, ZNF382 expression was analyzed with the online gene expression data extracted from http://kmplot.com/analysis (Fig. 1C). High expression of ZNF382 was able to significantly prolong patient survival time in the basal group. MSP results showed that ZNF382 CpG island was methylated in 59% (62/105) of breast cancer tissues and 25% (4/16) of breast adjacent tissues, respectively ($P < 0.05$) (Fig. S1 and Table 3). Furthermore, clinical feature analysis demonstrated that ZNF382 was more dramatically methylated in basal-like breast cancer tissues compare to lumina-type breast cancer tissues (Table 4), which consists of its expression. These data, combined with our previous reports, indicated that ZNF382 was highly expressed in normal breast tissues and downregulated or silenced in breast cancer tissues via promoter DNA methylation, suggesting that ZNF382 may be an independent prognostic factor of breast cancer.

ZNF382 overexpression inhibits breast cancer cells proliferation and colony formation

Stable expression of ZNF382 in MDA-MB231 and MCF7 cells, and ZNF382 knockdown in BT549 cell were confirmed by RT-PCR and western blotting (Fig. 2A, B). Cell proliferation was significantly suppressed in ZNF382 stably transfected MDA-MB231 and MCF7 cells compared to the control (Fig. 2C), while ZNF382 knockdown promoted BT549 cell growth (Fig. 2C). Colony formation assays showed that ectopic expression of ZNF382 inhibited cell colony formation in breast cancer cells (Fig. 2D).

ZNF382 induces G0/G1 cell cycle arrest and apoptosis in breast cancer cells

Ectopic expression of ZNF382 may suppress breast cancer cell proliferation by mediating cell cycle and apoptosis. Overexpression of ZNF382 significantly increased the quantity of MDA-MB231 and MCF7 cells in G0/G1 phase (Fig. 2E). Knockdown of ZNF382 expression in BT549 cells could lower cell cycle G0/G1 arrest which were measured by flow cytometry (Fig. S2). Cell apoptosis analyzed by flow cytometry showed that overexpression of ZNF382 in both

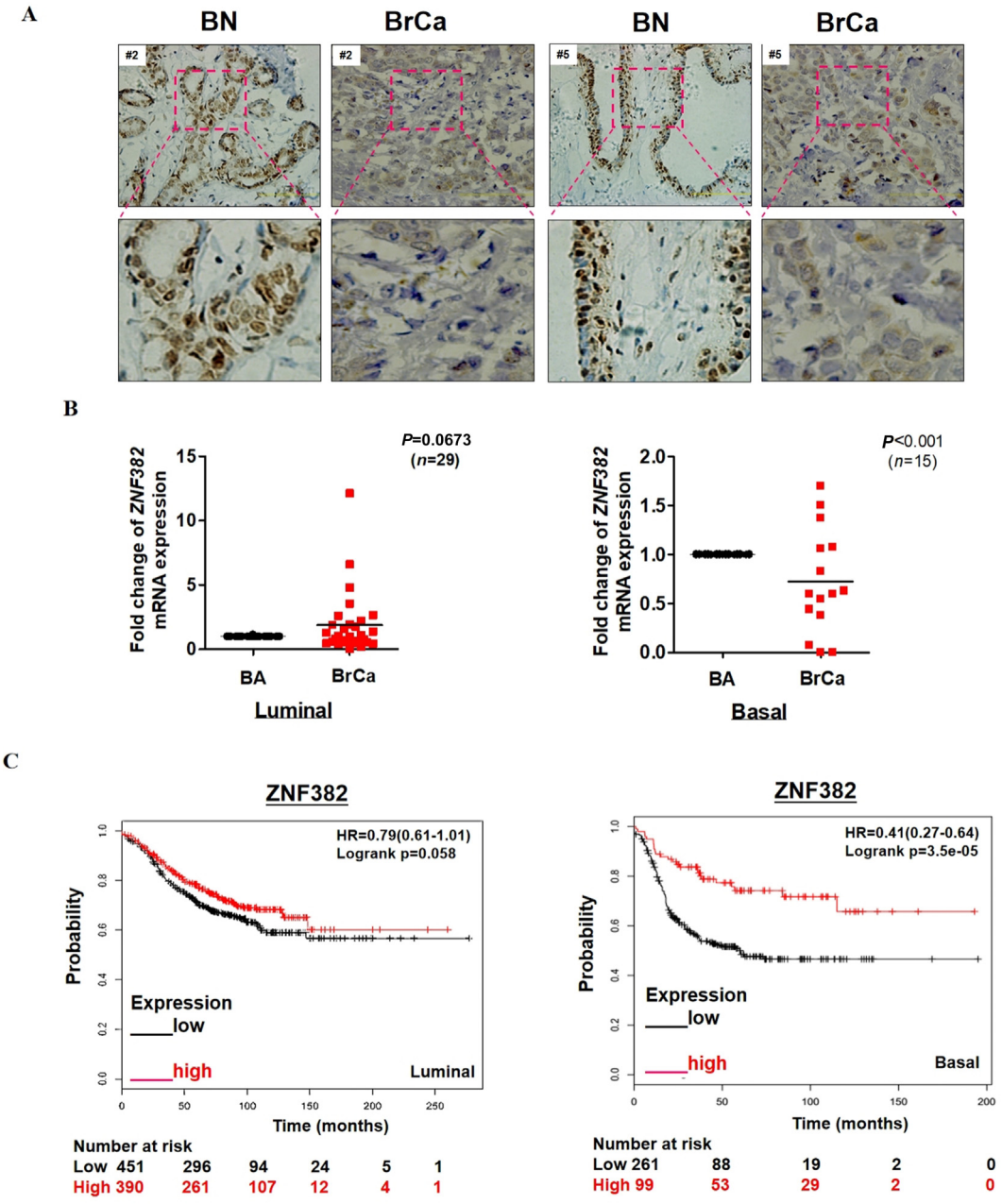

Figure 1 ZNF382 is downregulated in breast cancer tissues. **(A)** Immunohistochemical detection showed that ZNF382 is downregulated in breast cancer specimens compared to para-cancerous tissues. **(B)** Expression of ZNF382 in cancer and adjacent tissues was detected by qRT-PCR. **(C)** High expression of ZNF382 can significantly prolong patient survival time. Data were extracted from http://kmplot.com/analysis.

Table 3 Methylation status of ZNF382 promoter in primary breast tumors.

Samples	ZNF382		Frequency of Methylation
	Methylation	Unmethylation	
BrCa ($N = 105$)	62	43	62/105 (59%)
BA ($N = 16$)	4	12	4/16 (25%)

Note: BrCa, breast cancer; BA, breast adjacent tissues.

MDA-MB231 and MCF7 cells induced cell apoptosis compared to the control group (Fig. 2F).

ZNF382 inhibits wound healing, migration, and invasion in breast cancer cells, while ZNF382 knockdown promotes BT549 cell migration ability

The effect of ZNF382 on cell migration was investigated by using scratch wound healing assays. Experimental results

Table 4 ZNF382 promoter methylated status in BrCa.

Clinicopathological features	Number ($N = 105$)	Methylated	Unmethylated	*P* value
Age				0.304
≤40	19	10	9	
>40 < 65	73	42	31	
≥65	13	10	3	
Staging				0.463
I	2	1	1	
II	62	38	24	
III	22	10	12	
unknown	19	13	6	
Tumour size				0.553
<2.0 cm	38	25	13	
≥2.0 cm ≤ 5.0 cm	59	33	26	
>5.0 cm	8	4	4	
Lymph node metastasis				0.1938
present	25	9	16	
absent	61	34	27	
Distant Metastasis				0.566
present	3	1	2	
absent	102	61	41	
BrCa Type				**0.00841****
Lumina	45	20	25	
Basal-like	60	42	18	

showed that ZNF382 could suppress cell migration in ZNF382 stably transfected MDA-MB231 cells compared to the control group (Fig. 3A). Migration and invasion were further studied using the Transwell assay. Reduced numbers of migrating cells were found in MCF7 cell populations stably transfected with ZNF382 (Fig. 3B). ZNF382 knockout promoted the migration ability of BT549 cells (Fig. 3C). The matrigel invasion assay showed that over-expression of ZNF382 can suppress the invasive ability of MDA-MB231and MCF7 cells (Fig. 3D). These experimental results -manifest that ZNF382 can inhibit migration and invasion in breast cancer cells.

ZNF382 inhibits cell migration and invasion by regulating EMT

Immunofluorescence showed the localization of ZNF382 in MDA-MB231 cell (Fig. 4A). To investigate the underlying mechanisms of ZNF382 migration and invasion inhibition in breast tumor cells, the relationship between EMT-related genes and ZNF382 was studied with qPCR and western blotting (Fig. 4B, C). It was further verified that ectopic expression of ZNF382 in breast cancer cells negatively regulated the ZEB1 and SNAIL expression. In addition, Western blot results also showed that over-expression of ZNF382 can increase the epithelial marker E-Cadherin and Occludin expression levels and decrease the mesenchymal marker Vimentin, N-Cadherin and Slug expression levels compared to the control group. Four classical stem cell biomarkers were also decreased in ZNF382-overexpressing MDA-MB231 and MCF7 cells. Immunofluorescence assay was used to investigate the expression change in E-Cadherin and N-Cadherin after ZNF382 was transfected, suggesting the anti-EMT efficacy of ZNF382. These data showed that ZNF382 can inhibit EMT in breast cancer cells (Fig. 4D).

ZNF382 induces G0/G1 cell cycle arrest via CDC25A signaling pathway

ChIP-Seq data of HEK293 cells stably expressing eGFP-ZNF382 fusion protein were downloaded from the Gene Expression Omnibus (GEO) database. Enriched peaks located in the transcriptional start sites of CDC25A and ZEB1 genes were obtained, suggesting that CDC25A and ZEB1 are the direct targets of ZNF382. List of Chip-Seq peaks for ZNF382 targets were listed in our previous study.

Our previous functional experiments found ZNF382 plays an essential role in cell cycle regulation. Thus, several-cycle-related genes of candidate cell (CDC25A, CCND1, CCNB1, CCNE1, CDK1, CDK2, CDK4, CDK6 and C-Myc) expression were detected by qPCR in ZNF382 over-expression group and control group. The results showed that ZNF382 in breast cancer dramatically decreased the expression of CDC25A. Therefore, it was selected for further investigation (Fig. S3; Fig. 5A). Conversely, ZNF382 knockdown increased the expression of CDC25A in BT549 cells (Fig. 5B). In addition, recovery of CDC25A expression in breast cancer cell lines (MDA-MB231 and MCF7) partially antagonized the effect of ZNF382 on cell cycle arrest, especially in MCF7 cells (Fig. 5C). A mutual function between ZNF382 and CDC25A was elucidated as well in MDA-MB231 (Fig. 5D). Western blotting results revealed a connection between ZNF382 expression and cell

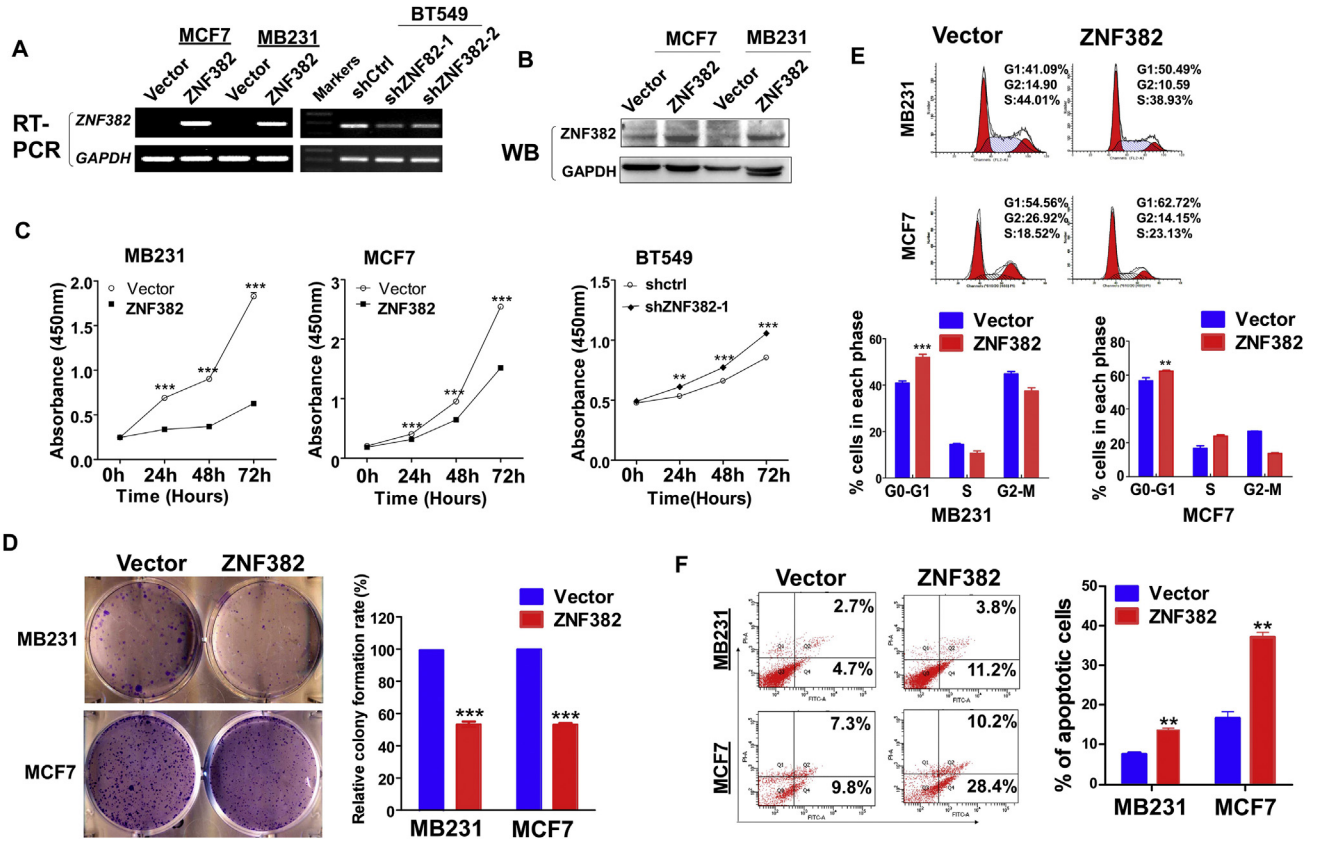

Figure 2 ZNF382 suppresses breast cancer cells proliferation and induces G2/M cell cycle arrest and apoptosis. **(A, B)** Ectopic expression of ZNF382 in MDA-MB231 and MCF7 cells and knock down ZNF382 in BT549 were confirmed by RT-PCR and Western blot, respectively. **(C)** CCK-8 assay was evaluated at 24, 48 and 72 h after transfection with ZNF382 in MDA-MB231 and MCF7 cells, and knockdown of ZNF382 in BT549 cells. **(D)** Representative images of showing the colony formation ability of in vector- and of ZNF382-transfected MDA-MB231 and MCF7 cells. **(E)** The cell cycle distribution was measured in vector- and ZNF382-stably transfected MDA-MB231 and MCF7 cells by flow cytometry analysis. Representative cell cycle distribution plots and histograms of cell cycle alterations are shown. **(F)** The percentages of apoptotic cells in MDA-MB231 and MCF7 cells with ZNF382 ectopic expression were evaluated. Cell apoptosis alterations were revealed by histograms. All experiments were performed in triplicate. Mean ± SD, $^{*}P < 0.05$, $^{**}P < 0.01$, $^{***}P < 0.001$.

cycle, and also indicated that ZNF382 significantly decreased the cleavage of CDC2, p-CDC2, CCND1 and C-Myc pathway in MDA-MB231 cells compared to the vector controls (Fig. 5E). To further validate CDC25A as the bona fide target gene of ZNF382, we performed ChIP assay on MCF7 cells, with a Flag antibody and PCR product spanning the identified ZNF382 binding sites. Indeed, ZNF382 was found to directly bind to the CDC25A promoter in breast cancer cells (Fig. 5F). Furthermore, dual-luciferase reporter assay confirmed that ZNF382 did decrease the activity of CDC25A (Fig. 5G).

ZNF382 regulates EMT by directly inhibiting ZEB1

Our previous functional experiments found that ZNF382 had a significant effect on cell EMT. Furthermore, ZEB1 is a key factor of EMT in breast cancer. Then, we verified that the expression of ZEB1 was decreased in over-expression of ZNF382 in MDA-MB231 and MCF7 cells by RT-PCR (Fig. 6A) and Western blotting (Fig. 6B). Based on the above, we performed ChIP assay to identified ZNF382 binding sites, and the results showed that ectopic expression of ZNF382 generated a significant decrease in enrichment of ZNF382 in the predicted region (binding sites 1 and 2). However, ChIP assay using IgG antibody as a negative control had no significant enrichment in the whole measured region (Fig. 6C, D). Moreover, dual-luciferase reporter assay revealed that ZNF382 expression dramatically inhibited ZEB1 promoter activity in MDA-MB231 and MCF7 cells (Fig. 6E). In addition, the recovery of ZEB1 expression partially antagonized the effect of ZNF382 on the ability of migration in MDA-MB231 cell (Fig. 6F, G). In summary, ZNF382 may regulate EMT by directly inhibiting the expression of ZEB1 in breast cancer cells.

ZNF382 inhibits xenograft tumor growth in nude mice

This study further explored whether ZNF382 can inhibit breast cancer cell growth *in vivo* using tumor formation in nude mice. MDA-MB231 cells transfected with pcDNA3.1-ZNF382-Flag or pcDNA3.1 plasmid were selected for

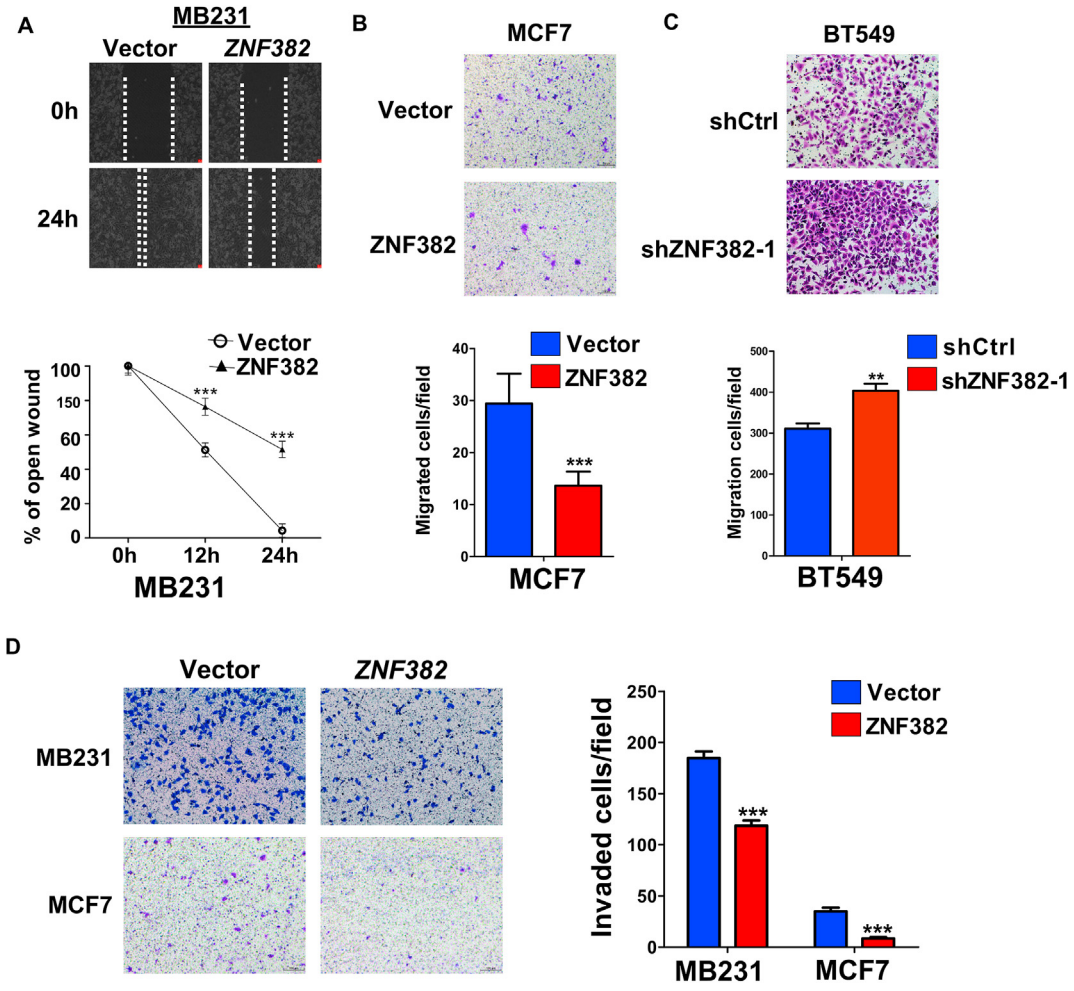

Figure 3 ZNF382 inhibits cell migration and invasion of breast cancer cells. **(A)** The cell migration abilities of MDA-MB231 cells were evaluated by wound healing assays. Photographs were captured at 0 and 24 h. **(B)** The cellular migration abilities of MCF7 cells upon ectopic expression of ZNF382 were measured by transwell assays without Matrigel. Representative images were photographed following fixation and staining. **(C)** Knockdown of ZNF382 promoted BT549 cell migration ability. Statistical charts with average values for (A–C) are shown below corresponding images. **(D)** Cellular invasion abilities of MDA-MB231 and MCF7 cells were examined using the Transwell assay with Matrigel (left). Invasion abilities were demonstrated using histogram statistical analysis (right). All images were obtained at magnification of 400 × . All experiments were performed in triplicate. Mean ± SD, $^{*}P < 0.05$, $^{**}P < 0.01$, and $^{***}P < 0.001$.

inoculation into subcutaneous tissue of five nude mice, and tumor size was measured every 2 days. After the nude mice were sacrificed by the end of day 20, the tumors were extracted and weighed. ZNF382 significantly inhibited the MDA-MB231 cell growth (Fig. 7A). Tumor weights in the ZNF382 over-expression group were significantly decreased compared to the control group (Fig. 7B). Tumor growth curves are shown in Figure 7C. ZNF382 over-expression was verified by IHC using xenograft tumor tissue slices harvested from nude mice and fixed in 10% buffered formalin for 24 h. H&E staining results were suggestive of a pro-EMT tendency in ZNF382 over-expression tumor samples. Furthermore, IHC results showed that ZNF382 could down-regulate the expression of CDC25A, Ki-67 and Vimentin, and up-regulate the expression of E-Cadherin in xenograft tumors. It suggested that the expression of ZNF382 is closely related to the proliferation of breast cancer and EMT *in vivo* (Fig. 7D).

Discussion

In present study, we found that ZNF382 was significantly reduced or silenced in breast cancer tissues compared to adjacent normal tissues, especially in basal-carcinoma. Functionally, ZNF382 inhibit breast cancer cell invasion and metastasis and induce G0/G1 phase cell cycle arrest and apoptosis. Moreover, ZNF382 could significantly inhibit the growth of MDA-MB231 cell xenograft tumors in nude mice. Mechanistically, ZNF382 could inhibit cell proliferation and colony formation via repressing CDC25A signaling. Further, ZNF382 negatively regulate

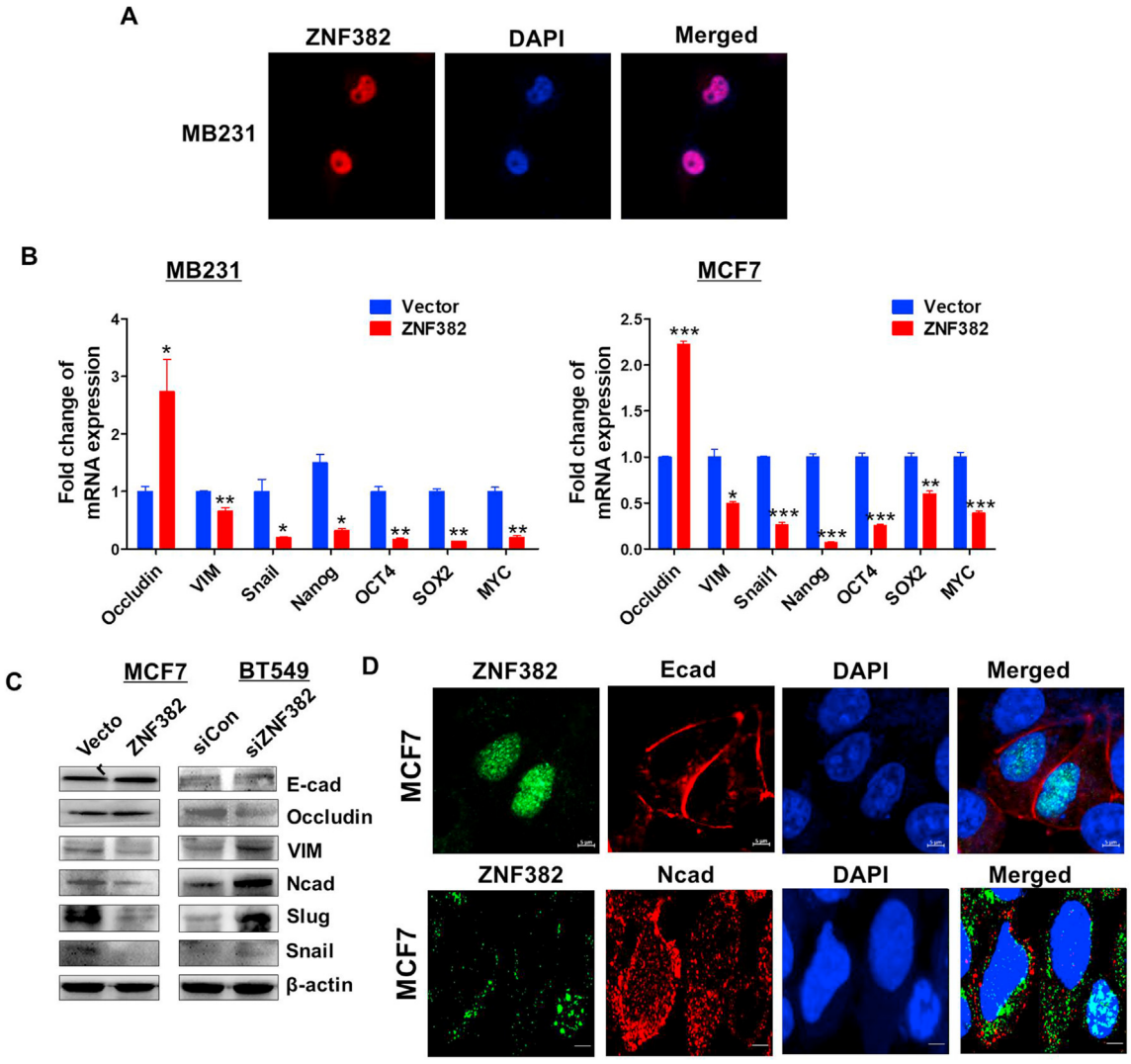

Figure 4 ZNF382 inhibits EMT and stem cell properties in breast tumor cells. **(A)** Locations of ZNF382 in MDA-MB231 cells was detected by immunofluorescence assay (400 × magnification). **(B)** EMT and stem cell markers in ZNF382 stably transfected MDA-MB231 and MCF7 cells were measured by qRT-PCR. **(C)** EMT-related markers in ZNF382-transfected MCF7 and ZNF382-knockout BT549 cells were measured by Western blot. **(D)** EMT markers in ZNF382-transfected MCF7 were measured by immunofluorescence staining. All experiments were performed in triplicate. Data are presented as the mean ± SD, $^{*}P < 0.05$, $^{**}P < 0.01$, and $^{***}P < 0.001$.

ZEB1 expression through directly binding to its promoter to inhibit EMT.

Previous reports have found that, Nanog, Sp1, KRAS, TP53, SMAD4 and TXN, as potential biomarkers, can be used for future cancer treatment.[5,20–22] However, more novel and valuable molecular targets for breast cancer still need to be excavated. KRAB-ZNFs belong to the largest families of regulatory transcription factors in mammals and play a key role in the formation of tumors.[23] However, little is currently known about the functions and target genes of KRAB-ZFPs in cancers, including breast cancer. Thus, investigating how cancer-associated KRAB-ZNFs factors function in cancer cells might be potential therapeutic strategies in breast cancer. The emerging evidence suggests that different KRAB-ZNFs genes may function as anti-oncogene or proto-oncogene in breast carcinogenesis.[24] Zinc finger E-box binding homeobox 1 (ZEB1) is an important proto-oncogene that participates in and adjusts the differentiation and metastasis of breast cancer cells.[25,26] ATM 53-associated KZNF protein (APAK) can specifically participate in p53-mediated apoptosis and negatively regulate the activity of tumor suppressor gene p53.[12,27] Our previous study also demonstrated that the KRAB-zinc-finger protein ZNF545 and BTB/POZ zinc finger protein ZBTB16 were potential suppressor gene and disrupted by promoter CpG methylation in breast tumor.[28,29] Several current research showed that ZNF382, as a member of KRAB-ZNFs, is an important suppressor. Reports showed that ZNF382 is frequently silenced in nasopharyngeal, gastric, and esophageal carcinomas via methylation.[13–15] It has been reported that abnormal methylation of the ZNF382 promoter region was observed in breast cancer, but its biological functions

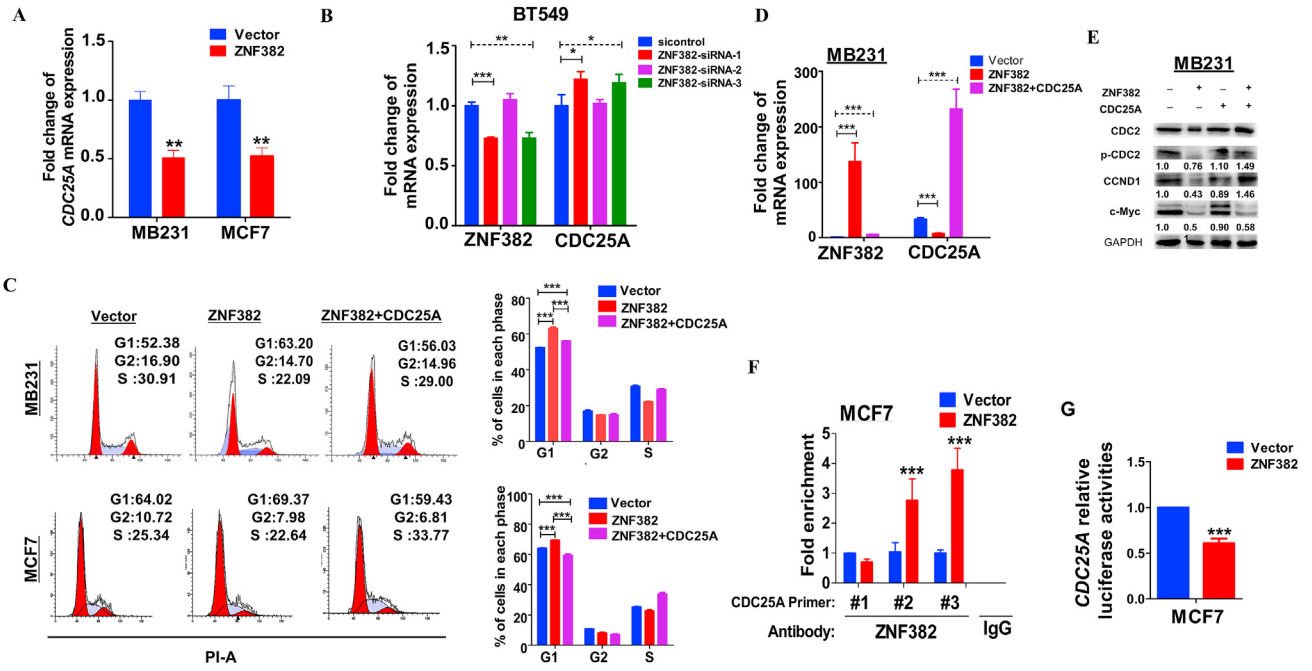

Figure 5 ZNF382 induces G0/G1 cell cycle arrest via CDC25A signaling pathway. **(A)** qRT-PCR showed that ZNF382 could decrease CDC25A expression. **(B)** qRT-PCR demonstrates that knockdown of ZNF382 in BT549 cells could up-regulate CDC25A expression. **(C)** Recovery of CDC25A expression in MDA-MB231 and MCF7 cells could antagonize ZNF382 effect on cell cycle arrest which were measured by flow cytometry (left). The effect on the cell cycle was demonstrated by histogram statistical analysis (right). **(D)** ZNF382 and CDC25A expression in vector, MDA-MB231 and MDA-MB231+ CDC25A cells were measured by qRT-PCR. **(E)** The expression of cleavage of CDC2, p-CDC2, CCND1 and C-Myc in ZNF382 transfected-MDA-MB231 cells were measured by Western blot. **(F)** Input % of CDC25A DNA by anti-Flag antibody were determined by ChIP-qPCR. **(G)** The effect of ZNF382 on CDC25A signaling, as determined by luciferase reporter activity assays. Data are presented as the mean ± SD, $^{*}P < 0.05$, $^{**}P < 0.01$, and $^{***}P < 0.001$.

and mechanisms remained unknown.[13] In our present study, we figured out the ZNF382 took part in the progress of breast cancers, restoration of ZNF382 expression could inhibit cell proliferation and colony formation. Moreover, ZNF382 could significantly inhibit the growth of MDA-MB231 cell xenograft tumors in nude mice.

Uncontrolled cell cycle regulation is well-known to be an important biological characteristic of tumor formation.[30] The current study found that ZNF382 expression restoration induced the G0/G1 cell cycle arrest. Moreover, we found that ZNF382 was significantly reduced or lost in basal-like breast carcinoma (BLBC), and the high expression of ZNF382 significantly correlated with better prognosis in BLBC. The report identified that BLBC tended to grow and spread quickly with aberrant expression of EMT markers and stemness markers.[31] EMT is an important biological process by which epithelial-derived malignant tumor cells acquire their ability to migrate and invade.[32] Also, EMT is closely related to stem cell characteristics of tumor cells.[33,34] The recovered ZNF382 gene expression significantly inhibited EMT and tumor stem cells factor expression, including NANOG, OCT4, Sox 2 and MYC. Through the cell function experiments, we found the ZNF382 dramatically reversed EMT process and promoted mesenchymal–epithelial transition in breast cancer xenografts in nude mouse, as well as diminishing expression of stemness markers.

Based on our data, we identified two target genes, CDC25A and ZEB1, from ChIP Sequence of HEK293 cells stably transfected with ZNF382. As an oncogene, CDC25A is necessary for cell progression from G1 to S phase via activating cyclin-dependent kinase CDC2. In our study, ZNF382 down-regulated the activity of CDC25A was confirmed by ChIP assay and dual-luciferase reporter assay in breast cancer cells, which suggested that G0/G1 cell cycle arrest was associated with deregulation of CDC25A signaling pathway. The recovery of CDC25A expression partially antagonized the effect of ZNF382 on cell cycle arrest. Therefore, it was speculated that ZNF382 can inhibit cell cycle in breast cancer cells by down-regulating CDC25A.

Furthermore, we verified that ZNF382 could negatively regulate ZEB1 through ChIP assay and luciferase reporter assay. As we all known, ZEB1 is a crucial inducer of EMT in breast cancer.[25,26,35] Previous reports found that ZEB1 triggers an microRNA-mediated feed forward loop that stabilizes EMT and promotes invasion of breast cancer cells.[36] Therefore, we speculated that, as a transcription factor, ZNF382 may negatively regulate ZEB1 by binding to the promoter region, which inhibited EMT in breast cancer cells.

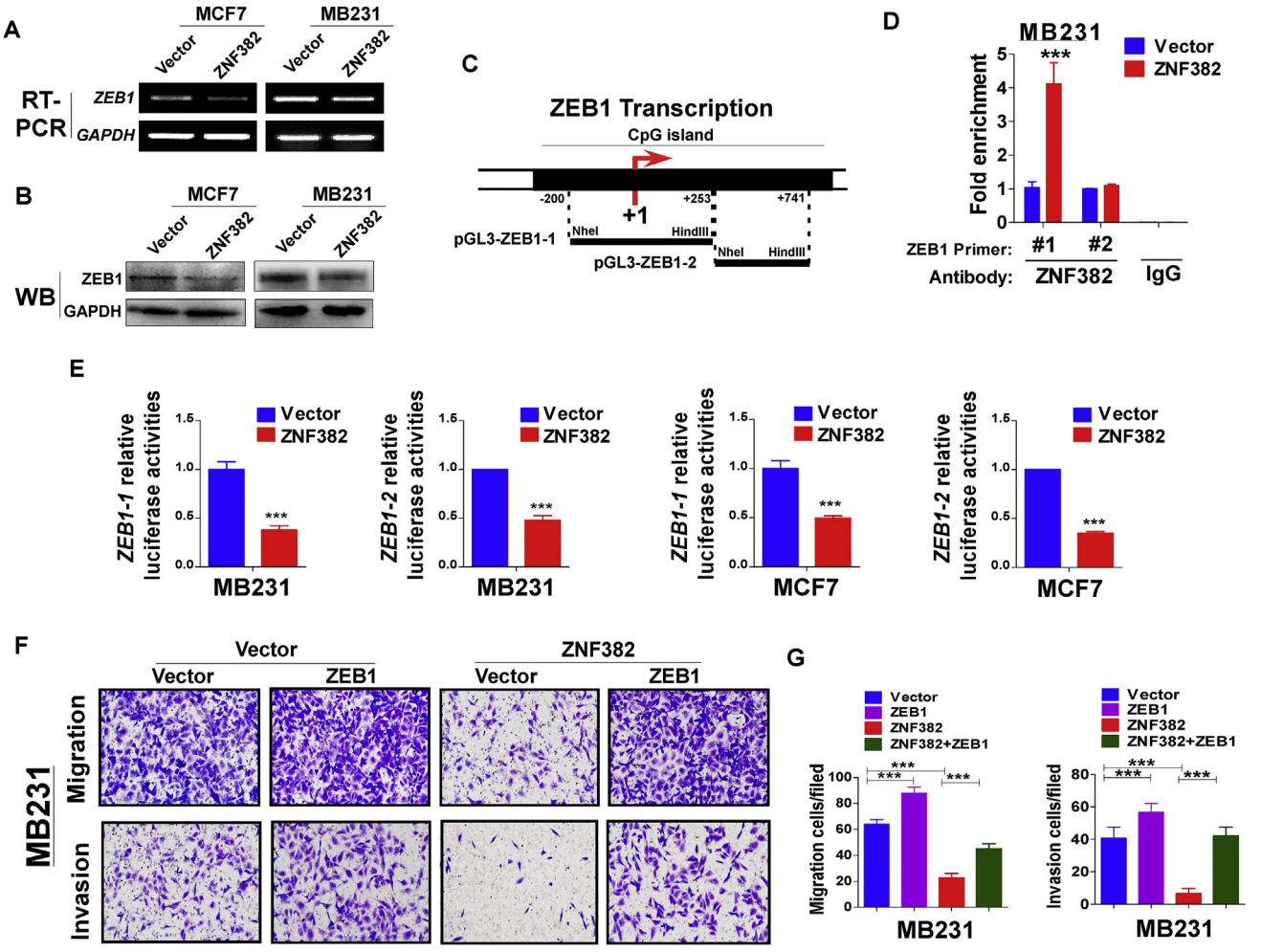

Figure 6 *ZNF382* regulates EMT by directly inhibiting ZEB1. **(A, B)** The expression of ZEB1 in ZNF382 stably transfected MDA-MB231 and MCF7 cells was measured by RT-PCR and Western blot. **(C)** The pLG3-ZEB1-1 plasmid corresponds to segment 1 (-200-+253), and the pLG3-ZEB1-2 plasmid corresponds to segment 2 (+254-+741). **(D)** Input% of ZEB1 DNA by anti-Flag antibody were determined by ChIP-qPCR. **(E)** The effect of ZNF382 on ZEB1 was determined by luciferase reporter activity assays. **(F)** Recovery of ZEB1 expression antagonize the effect of ZNF382 on the ability of migration in MDA-MB231×cells, 200 × magnification. **(G)** Migration abilities were measured by histogram statistical analysis in ZNF382-infected MDA-MB231 and MCF7 cells after over expression ZEB1. Data are presented as the mean ± SD, ***$P < 0.001$.

Our previous studies found that the different expression of ZNF382 may be related to the molecular type of breast cancer. There is a decreased tendency in lumila A type breast cancer with the expression of ZNF382, limited by clinical sample, we could not get a valid conclusion. Therefore, for the subsequent studies, we should expand the sample numbers to explore more clinical significance of ZNF382 in breast cancers. Our studied mainly focus on the downstream regulation of ZNF382 and the specific biological mechanism on methylation of ZNF382 needs to be further explored. With the development of tumor molecular biology research, demethylation drugs and cell cycle inhibitors (CDK4/6) play an important role in the treatment of breast cancer patients. In this study, ZNF382 was also found to inhibit CDC25A, thereby regulating the cell cycle. To further find more targets for the precise treatment of breast cancer, we can explore the correlation between ZNF382 and drugs mentioned above and uncover the key mechanisms in the occurrence and development of different molecular types of breast cancer.

In conclusion, ZNF382 is often silenced in breast cancer and can inhibit tumor cell proliferation by directly suppressing cell cycle correlation factor CDC25A, meanwhile, it can also inhibit cell migration and invasion via regulating EMT by inhibiting ZEB1. Our results indicated that ZNF382 may be a potential target for breast cancer molecular therapy and the further studies focusing on then mechanisms responsible for ZNF382 methylation in breast cancer are required.

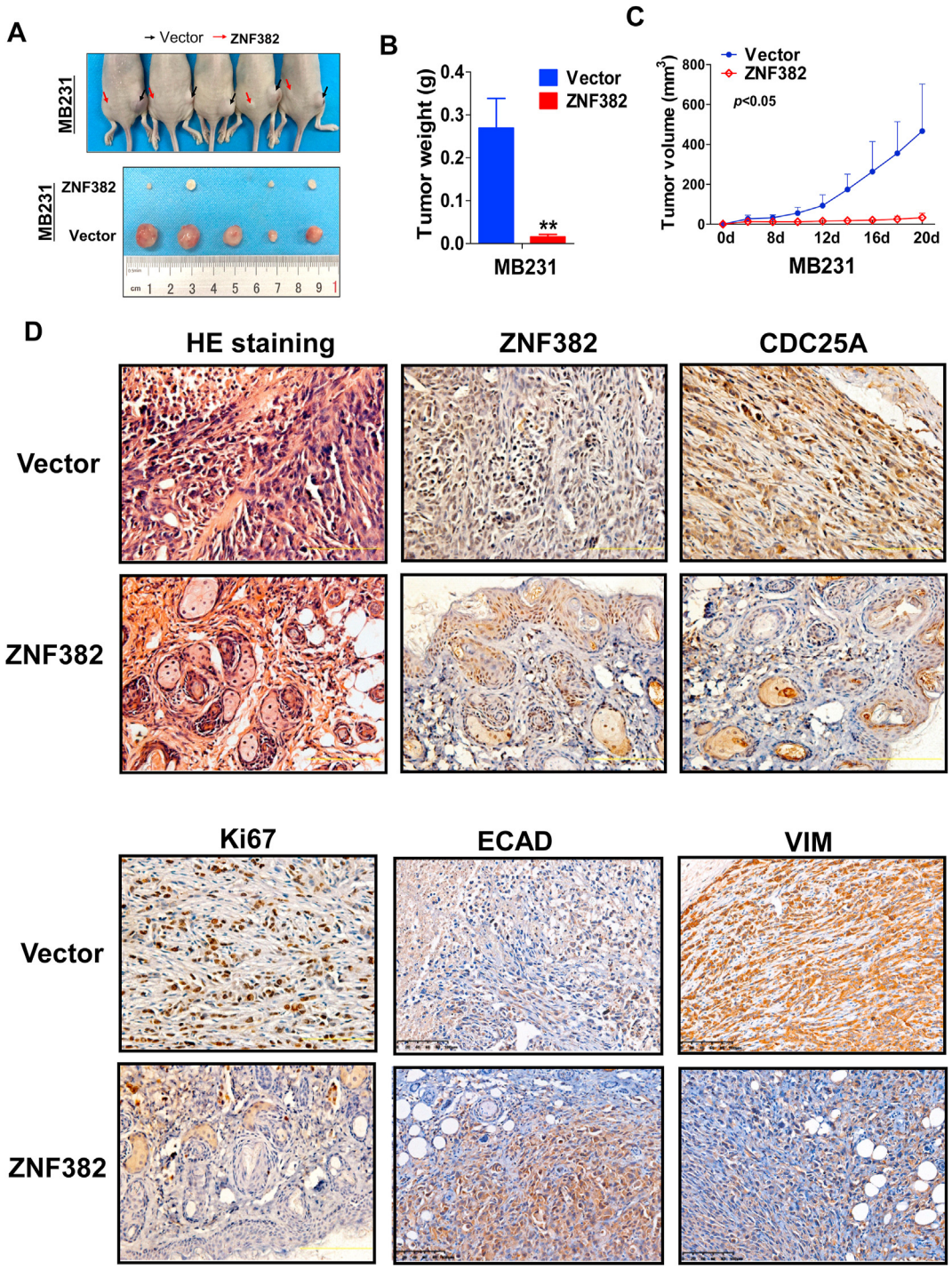

Figure 7 ZNF382 inhibits xenograft tumor growth in nude mice. **(A)** Images of human breast tumor xenografts. **(B)** Comparative histogram of tumor weights in the two groups (empty vector group *vs.* stably expressing ZNF382 group) of nude mice. **(C)** Comparative analyses of tumor growth curve for vector- and ZNF382-transfected MDA-MB231 cells in nude mice xenografts. **(D)** Representative photographs of H&E staining and IHC expression analyses of ZNF382, CDC25A, Ki-67, E-Cadherin and Vimentin in xenografts (400 × magnification). Mean ± SD, $^{*}P < 0.05$, $^{**}P < 0.01$, and $^{***}P < 0.001$.

Data availability

All data generated or analyzed during this study are included in this published article (and its supplementary information files).

Author contributions

TX: conception and design. SL, XH, YW, DZ, YJ, SR: performed majority of experiments. TX, SL, XH: performed experiments and analyzed data. SH, ST, CP, CL: collected

samples. TX, SL, LL: drafted the manuscript. TX, QT, XH: reviewed data and manuscript. TX, SL: reviewed data and finalized the manuscript. All authors reviewed and approved the final version.

Conflict of interests

The authors declare no conflict of interest.

Funding

This study was supported by National Natural Science Foundation of China (No. 81872380, 81772869), Natural Science Foundation of Chongqing (No. 2019ZX002, cstc2019jcjy-msxmX0861, cstc2020jcyj-bshX0025) and Opening Foundation of Chongqing Key Laboratory of Molecular Oncology and Epigenetics (No. MOEL201702), Postdoctoral Science Fundation of China (No. 2020M683262), National Key Research and Development Program of China (No. 2017YFE01 91700) and HK RGC (No. GRF14115019).

Appendix A. Supplementary data

Supplementary data to this article can be found online at https://doi.org/10.1016/j.gendis.2021.12.019.

References

1. Siegel RL, Miller KD, Jemal A. Cancer statistics. *CA Cancer J Clin*. 2020;70(1):7—30, 2020.
2. Kono M, Fujii T, Lim B, et al. Androgen receptor function and androgen receptor—targeted therapies in breast cancer: a review. *JAMA Oncol*. 2017;3(9):1266—1273.
3. Waks AG, Winer EP. Breast cancer treatment: a review. *JAMA*. 2019;321(3):288—300.
4. Goutsouliak K, Vidyalakshmi S, Carmine DA, et al. Towards personalized treatment for early stage HER2-positive breast cancer. *Nat Rev Clin Oncol*. 2020;17(4):233—250.
5. Saranya T, Kavithaa K, Paulpandi M, et al. Enhanced apoptogenesis and oncogene regulatory mechanism of troxerutin in triple negative breast cancer cells. *Toxicol Res (Camb)*. 2020;9(3):230—238.
6. Hu X, Fan M. Emerging therapies for breast cancer. *J Hematol Oncol*. 2017;10(1):98.
7. Bianchini G, Balko JM, Mayer IA, et al. Triple-negative breast cancer: challenges and opportunities of a heterogeneous disease. *Nat Rev Clin Oncol*. 2016;13(11):674—690.
8. Garrido-Castro AC, Lin NU, Polyak K. Insights into molecular classifications of triple-negative breast cancer: improving patient selection for treatment. *Cancer Discov*. 2019;9(2):176—198.
9. Penault-Llorca F, Radosevic-Robin N. Biomarkers of residual disease after neoadjuvant therapy for breast cancer. *Nat Rev Clin Oncol*. 2016;13(8):487—503.
10. Margolin JF, Friedman JR, Meyer WK, et al. Kruppel-associated boxes are potent transcriptional repression domains. *Proc Natl Acad Sci U S A*. 1994;91(10):4509—4513.
11. Huntley S, Baggott DM, Hamilton AT, et al. A comprehensive catalog of human KRAB-associated zinc finger genes: insights into the evolutionary history of a large family of transcriptional repressors. *Genome Res*. 2006;16(5):669—677.
12. Tian C, Xing G, Xie P, et al. KRAB-type zinc-finger protein Apak specifically regulates p53-dependent apoptosis. *Nat Cell Biol*. 2009;11(5):580—591.
13. Cheng Y, Geng H, Cheng SH, et al. KRAB zinc finger protein ZNF382 is a proapoptotic tumor suppressor that represses multiple oncogenes and is commonly silenced in multiple carcinomas. *Cancer Res*. 2010;70(16):6516—6526.
14. Zhang C, Xiang T, Li S, et al. The novel 19q13 KRAB zinc-finger tumour suppressor ZNF382 is frequently methylated in oesophageal squamous cell carcinoma and antagonises Wnt/beta-catenin signalling. *Cell Death Dis*. 2018;9(5):573.
15. Pei L, Li S, Sun R, et al. KRAB zinc-finger protein 382 regulates epithelial-mesenchymal transition and functions as a tumor suppressor, but is silenced by CpG methylation in gastric cancer. *Int J Oncol*. 2018;53(3):961—972.
16. Dang S, Chen Y, Chen P, et al. Dynamic expression of ZNF382 and its tumor-suppressor role in hepatitis B virus-related hepatocellular carcinogenesis. *Oncogene*. 2019;38(24):4804—4819.
17. Tao YF, Hu SY, Lu J, et al. Zinc finger protein 382 is downregulated by promoter hypermethylation in pediatric acute myeloid leukemia patients. *Int J Mol Med*. 2014;34(6):1505—1515.
18. Xiang T, Tang J, Li L, et al. Tumor suppressive BTB/POZ zinc-finger protein ZBTB28 inhibits oncogenic BCL6/ZBTB27 signaling to maintain p53 transcription in multiple carcinogenesis. *Theranostics*. 2019;9(26):8182—8195.
19. Xiang T, Fan Y, Li C, et al. DACT2 silencing by promoter CpG methylation disrupts its regulation of epithelial-to-mesenchymal transition and cytoskeleton reorganization in breast cancer cells. *Oncotarget*. 2016;7(43):70924—70935.
20. Lyer M, Mohana DS, Kaavya J, et al. New insight into NANOG: a novel therapeutic target for ovarian cancer (OC). *Eur J Pharmacol*. 2019;5(852):51—57.
21. Vellingiri B, Lyer M, Mohana MD, et al. Understanding the role of the transcription factor Sp1 in ovarian cancer: from theory to practice. *Int J Mol Sci*. 2020;21(3):1153.
22. Kaavya J, Verllingiri B, Kumaran SS. Ampullary carcinoma-A genetic perspective. *Mutat Res Rev Mutat Res*. 2018:77610—77622.
23. Lupo A, Cesaro E, Montano G, et al. KRAB-zinc finger proteins: a repressor family displaying multiple biological functions. *Curr Genom*. 2013;14(4):268—278.
24. Machnik M, Cylwa R, Kielczewski K, et al. The expression signature of cancer-associated KRAB-ZNF factors identified in TCGA pan-cancer transcriptomic data. *Mol Oncol*. 2019;13(4):701—724.
25. Liu L, Tong Q, Liu S, et al. ZEB1 upregulates VEGF expression and stimulates angiogenesis in breast cancer. *PLoS One*. 2016;11(2):e0148774.
26. Zhang P, Wei Y, Wang L, et al. ATM-mediated stabilization of ZEB1 promotes DNA damage response and radioresistance through CHK1. *Nat Cell Biol*. 2013;16(9):864—875.
27. Wang S, Tian C, Xing G, et al. ARF-dependent regulation of ATM and p53 associated KZNF (Apak) protein activity in response to oncogenic stress. *FEBS Lett*. 2010;584(18):3909—3915.
28. Xiang S, Xiang T, Xiao Q. Zinc-finger protein 545 is inactivated due to promoter methylation and functions as a tumor suppressor through the Wnt/beta-catenin, PI3K/AKT and MAPK/ERK signaling pathways in colorectal cancer. *Int J Oncol*. 2017;51(3):801—811.
29. He J, Wu M, Xiong L, et al. BTB/POZ zinc finger protein ZBTB16 inhibits breast cancer proliferation and metastasis through upregulating ZBTB28 and antagonizing BCL6/ZBTB27. *Clin Epigenet*. 2020;12(1):82.
30. Otto T, Sicinski P. Cell cycle proteins as promising targets in cancer therapy. *Nat Rev Cancer*. 2017;17(2):93—115.

31. Sarrió D, Rodriguez-Pinilla SM, Hardisson D, et al. Epithelial-mesenchymal transition in breast cancer relates to the basal-like phenotype. *Cancer Res*. 2008;68(4):989—997.
32. Ko YS, Lee WS, Panchanathan R, et al. Polyphenols from artemisia annua L inhibit adhesion and EMT of highly metastatic breast cancer cells MDA-MB-231. *Phytother Res*. 2016; 30(7):1180—1188.
33. Kong D, Li Y, Wang Z, Sarkar FH. Cancer stem cells and epithelial-to-mesenchymal transition (EMT)-Phenotypic cells: are they cousins or twins? *Cancers*. 2011;3(1):716—729.
34. Marie-Egyptienne DT, Lohse I, Hill RP. Cancer stem cells, the epithelial to mesenchymal transition (EMT) and radioresistance: potential role of hypoxia. *Cancer Lett*. 2013;341(1): 63—72.
35. Gregory PA, Bert AG, Paterson EL, et al. The miR-200 family and miR-205 regulate epithelial to mesenchymal transition by targeting ZEB1 and SIP1. *Nat Cell Biol*. 2008;10(5):593—601.
36. Burk U, Schubert J, Wellner U, et al. A reciprocal repression between ZEB1 and members of the miR-200 family promotes EMT and invasion in cancer cells. *EMBO Rep*. 2008;9(6):582—589.